



# A new energy-positive technological approach for wastewater treatment and bioenergy generation using a photo anoxic baffled reactor (PABR)

M. Hasan<sup>1</sup> · Md. Khalekuzzaman<sup>1</sup> · M. Alamgir<sup>1</sup> · P. Datta<sup>1</sup> · S. B. Kabir<sup>1</sup>

Received: 4 July 2020 / Revised: 15 November 2020 / Accepted: 23 January 2021 / Published online: 15 February 2021  
© The Author(s) 2021

## Abstract

This study proposed a new energy-positive technological approach for wastewater treatment and bioenergy generation using an algal–bacterial symbiosis system in a photo anoxic baffled reactor (PABR). The PABR consisted of a sedimentation chamber, four regular baffled chambers, and two floated filter media chambers. The PABR was operated in the presence of natural sunlight with an average intensity of 30  $\mu\text{moles}/\text{m}^2/\text{s}$ . A wide range of ORP (–215 to 255 mV) data suggested that a suitable environment condition existed in the PABR for photosynthesis, nitrification, and denitrification. Simultaneous nitrification/denitrification (SND) was observed in the first three chambers, and microbial assimilation was governed in the last four chambers. An average biochemical oxygen demand (BOD),  $\text{NH}_3\text{-N}$ , total nitrogen (TN), and  $\text{PO}_4^{3-}$  removal efficiencies were more than 88, 48, 36, and 42%, respectively. Moreover, hydrothermal liquefaction (HTL) was carried out for sludge and microalgae samples for bioenergy (e.g., biocrude and biochar) conversion, where the sludge sample containing microalgae and bacteria was collected from PABR and microalgae sample was collected from photobioreactor. Finally, the Fourier transform infrared spectroscopy (FTIR) analysis was done for both biocrude and biochar derived from sludge and microalgae samples, and it was suggested that the biocrude and biochar derived from sludge sample were better than that of microalgae sample.

**Keywords** Photosynthesis · PABR · Algal–bacterial culture · Biocrude · Biochar

## Introduction

As Bangladesh is located in the subtropical/tropical region with a warm climate (15–35 °C), the biological wastewater treatment process would be the best option for wastewater management. Recently, the anaerobic processes of wastewater treatment have been gained special attention among the researchers due to economic and environmental benefits over conventional aerobic treatment (Khalekuzzaman et al. 2019). Anaerobic treatment of wastewater is very suitable for low-strength wastewaters such as domestic wastewater, and satisfactory removal efficiencies are to be observed

(Kassab et al. 2010; Chen et al. 2014). Other advantages are: (a) zero consumption of oxygen which cuts down the cost of energy requirement, (b) very low sludge production that reduces the sludge handling cost, (c) biogas recovery, (d) low maintenance cost, and (e) high solids retention time at low hydraulic retention time (Gopala Krishna et al. 2009; Feng et al. 2009).

Among all high-rate anaerobic reactors, the anaerobic baffled reactor (ABR) is extensively used in treating wastewater. Initially, it was developed by McCarty and co-workers at Stanford University, and it can be described as a series of up-flow anaerobic sludge blanket reactors (UASBs) (Rongrong et al. 2010). The ABR has several numerous advantages over other reactors due to the unique compartmentalized structure, which is capable of separating anoxic denitrification and aerobic nitrification in the same reactor (Barber and Stuckey, 2000a). The other advantages are no special arrangement for gas and sludge separation, lower sludge yields, longer biomass retention times (SRT), lower hydraulic retention time (HRT), and its ability to separate

Editorial responsibility: Mohamed F. Yassin.

✉ M. Hasan  
mhasan12@ce.kuet.ac.bd

<sup>1</sup> Department of Civil Engineering, Khulna University of Engineering and Technology (KUET), Khulna, Bangladesh

acidogenesis and methanogenesis process longitudinally down the reactor (Langenhoff et al. 2000; Kuşçu and Sponza, 2005; Feng et al. 2008; Mohd Aris et al. 2016).

The major drawbacks of the anaerobic systems are the high concentration of nutrients and sulfur in the treated effluent (Alcántara et al. 2015; Zhu et al. 2015). The continuous discharge of such effluent in the natural water body without adequate treatment may cause severe eutrophication in aquatic ecosystems—the enrichment of nutrients (mainly nitrogen and phosphorus) in the water. In such a way, high levels of nutrients entering into the natural water body are responsible for the growth of algal blooms, spread of aquatic plants, and oxygen depletion, resulting in toxic conditions for wildlife (Saby et al. 2003; Sabumon, 2008; Wu et al. 2016). In order to protect the aquatic ecosystems, a reduction of nitrogen and phosphorus concentrations from the wastewaters before discharging into the natural water bodies is required for a sustainable sanitation system for meeting SDGs by 2030 in Bangladesh.

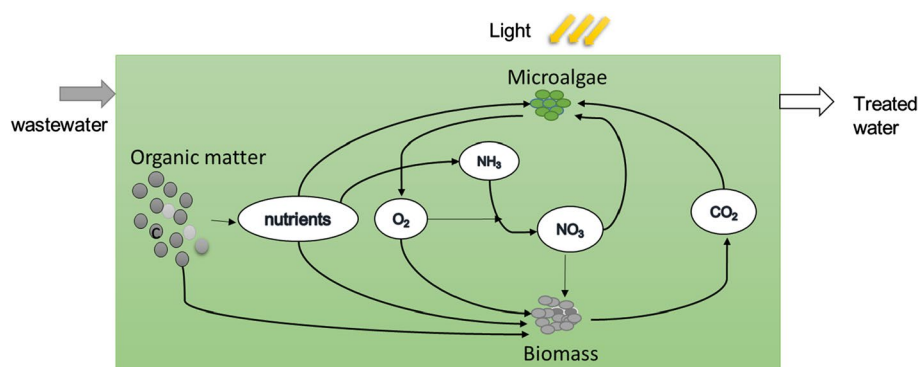
Therefore in recent years, special attention has been paid to conventional biological nutrient removal (BNR) processes that are based on microalgae–bacteria consortia systems would be an alternative technology with high nutrient removal efficiencies and nutrient recover possibilities (Rada-Ariza et al. 2017). The dual action of microalgae and nitrifying bacteria can reduce nutrient concentration through the process of assimilation and nitrification (Rada-Ariza et al. 2019). The advantage of using microalgae in the biological wastewater treatment process is that microalgae have an excellent affinity to uptake excess nitrogen (N) and phosphorus (P) through biomass assimilation (Lee and Lei, 2019). Although many traditional methods use chemicals to remove nitrogen, these methods are costly and release toxic compounds to the environment. Therefore, the development of algal–bacterial granules is considered as sustainable techniques for wastewater treatment as no energy is required for oxygen supply due to the photosynthetic oxygen production of microalgae (Tiron et al. 2017; He et al. 2018a, b). A general framework of organic matter and nutrient removal

technique by microalgal–bacterial symbiosis is depicted in Fig. 1.

During the treatment process, photosynthesis by microalgae produces oxygen and consumes carbon dioxide. This activity is beneficial in the biological wastewater treatment process since the oxygen produced by microalgae can be used by aerobic bacteria to degrade the organic matters and produce carbon dioxide that can be used by microalgae for photosynthesis (Medina and Neis, 2007; Boelee et al. 2012; Delgadillo-Mirquez et al. 2016). As photosynthesis activities take place between the microalgae and bacteria so no external supply of oxygen is required. Because the oxygen supplied by microalgae is used bacteria and the carbon dioxide produced by bacteria is used microalgae. Thus the photosynthesis cycle involves no cost for aeration during the treatment process in the PABR. Moreover, the microalgal–bacterial aggregate has good settling properties, which allow operating the system at low hydraulic retention time (HRT) without the risk of biomass washout (Nguyen et al. 2019). Also, filter media was used in last two chambers of the PABR to avoid the microalgae washout.

Recently, Khalekuzzaman et al. (2018a, b) have reported the existence of anoxic/aerobic conditions inside the anaerobic baffled reactor (ABR), which is a suitable environment for nitrogen removal without cost involvement. Besides, no external electron donor is required for denitrification as COD is present in the reactor acting as an electron donor that will actually improve COD removal performance by oxidizing a fraction of the COD in order to reduce nitrate (Barber and Stuckey, 2000b). Moreover, the microalgae–bacteria (sludge) harvested after wastewater treatment can be further used for bioenergy production as microalgae is a promising approach for future renewable energy sources (Quijano et al. 2017). In that case, the hydrothermal liquefaction (HTL) is the best alternative option to convert wet microalgae–bacteria into bioenergy at temperatures of 200–350 °C. Not only lipids but also proteins and carbohydrates can be converted into biocrude and biochar during the HTL process (Ponnuwamy et al. 2013; Guo et al. 2015). However, very little information is available on the process of HTL of PABR

**Fig. 1** Organic matter and nutrients removal by algal–bacterial symbiosis system



sludge and the characteristics of these products. So experiments were performed in a batch reactor, and a comparison between the microalgae and sludge samples was studied.

The microalgae–bacteria consortium is a sustainable and cost-effective approach for domestic wastewater treatment in developing countries like Bangladesh. However, there is no significant information available on the process of algal–bacterial symbiosis into the PABR. The process of algal–bacterial symbiosis was significantly affecting the nutrients removal performance on the photo anoxic baffled reactor (PABR). Therefore, the present research aimed to investigate the combined effect of microalgae–bacteria consortium in removing nutrient and organic matter and renewal use of sludge as a form of bioenergy.

## Materials and methods

### Reactor configuration

A laboratory scale of photo anoxic baffled reactor (PABR) was designed for the current study constructing with clear acrylic plastic. The proposed PABR configuration was the modification of the conventional anaerobic baffled reactor (ABR) by operating in the presence of natural sunlight. The schematic diagram of the proposed PABR is shown in Fig. 2, and the physical properties of the PABR are summarized in

Table 1. The external dimensions of the PABR were 90, 20, and 30 cm for length, width, and depth, respectively. The effective volume of the reactor was 36 L. The PABR consisted of one front sedimentation chamber (ch-1), four regular baffled chambers (ch-2–ch-5) followed by two floated filter media chambers (ch-6 and ch-7). The volume of the sedimentation chamber (ch-1) was twice than other chambers. The reactor was rectangular, containing standing baffle, hanging baffle, and inclined baffle. The standing baffles divided the reactor into seven identical compartments. The hanging baffles which were designed in each compartment were divided into two portions, such as down-comer and up-comer zone. The ratio of the up-comer and the down-comer zone was 4:1, and the lower part of the hanging baffle was bent at 45° (called inclined baffle) to route the flow to the center of the up-comer chamber, thus achieving better contact and greater mixing among the substrate and biomass. The last two chambers of the reactor were loosely packed with floated filter media such as shredded plastic soft drink lid (approximately 400 g) to reduce solid wash out. These filtered media are locally available, having a high specific surface area and less possible of clogging during wastewater treatment as specific gravity (0.93) is less than water.

**Fig. 2** The configuration of PABR (1—feeding tank, 2—peristaltic pump, 3—influent, 4—sampling port, 5—sedimentation chamber, 6—standing baffled, 7—hanging baffled, 8—floated filter media, 9—effluent)

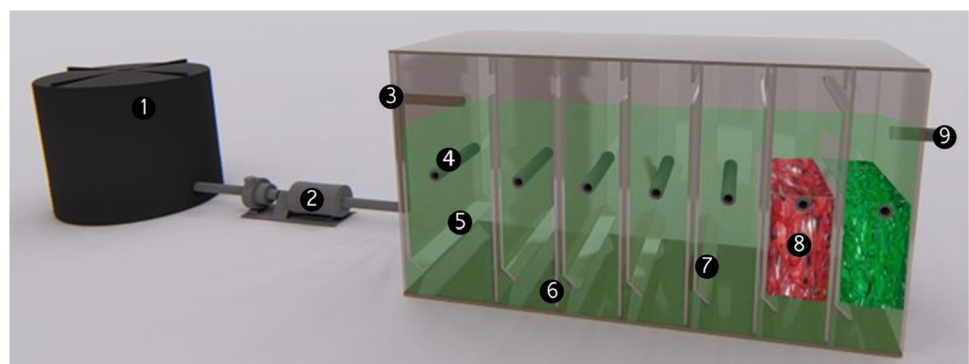


**Table 1** Physical parameters of the PABR

PABR compartment	Length (cm)	Width (cm)	Effective height (cm)	Volume (L)	Up-comer/Down-comer ratio
Ch-1	20	18.5	24	8.9	4:1
Ch-2	10	18.5	24	4.4	
Ch-3	10	18.5	24	4.4	
Ch-4	10	18.5	24	4.4	
Ch-5	10	18.5	24	4.4	
Ch-6	11	18.5	24	4.8	
Ch-7	11	18.5	24	4.8	
Sum = 36 L					

## Reactor operation

The system was set up at the roof of the Civil Engineering Building, KUET (Khulna University of Engineering and Technology, Khulna, Bangladesh) to provide sufficient sunlight during the entire experiment. The PABR was operated under ambient temperature ( $29.7 \pm 4.2$  °C) during the day with light irradiation of  $34 \pm 4.8$   $\mu\text{moles}/\text{m}^2/\text{s}$  at morning,  $26 \pm 5.2$   $\mu\text{moles}/\text{m}^2/\text{s}$  at noon, and  $14 \pm 4.2$   $\mu\text{moles}/\text{m}^2/\text{s}$  at afternoon, respectively, at the outer wall of the PABR. Domestic wastewater was collected from the residential area of the KUET campus and stored at a feeding tank, which was equipped at a mixture pump for uniform feeding. The feeding tank was loaded every 15 days interval. The characteristics of raw domestic wastewater and effluent water are summarized in Table 2. The PABR was then fed by a peristaltic pump (WT600-1F, Longer pump Co., China) and was running the system 10 min in every hour, which was maintained by a Sino-timer (Sino timer, China). During the experiment, the hourly flow rate was 1.2 L for 30 h HRT.

## Reactor inoculation

In the beginning, the PABR was inoculated with anaerobic septic sludge collected from the KUET residential area. Approximately 9 L of sieved sludge (using 2.0 mm mesh) was added to the reactor (3.0 L in the first chamber and 1.5 L in chamber 2–5), the remaining volume being filled with the effluent of septic tank including the chambers 6 and 7. The seeded sludge was containing total suspended solids (TSS) of  $8960 \pm 1824$  mg/L and volatile suspended solids (VSS) of  $6880 \pm 1137$  mg/L with a VSS/TSS ratio of 0.77. After inoculation, the reactor was allowed to stabilize at ambient temperature for 30 days without further modification. As septic tank effluent was used to inoculate the reactor so native microalgae species were grown automatically inside the reactor. Two major microalgae species of *Chlorella sp.* and *Scenedesmus sp.* were identified with the help of microscope at a magnification of 40x.

**Table 2** Characteristics of raw and effluent sample

Parameter	Unit	Raw	Effluent
pH	–	$8.1 \pm 0.2$	$8.1 \pm 0.1$
EC	mS/cm	$2.62 \pm 0.06$	$2.53 \pm 0.14$
Turbidity	NTU	$414.6 \pm 224.2$	$6.74 \pm 4.4$
TN	mg/L	$79.5 \pm 12.6$	$50.2 \pm 6.0$
$\text{NH}_3 - \text{N}$	mg/L	$67.7 \pm 12.7$	$34.9 \pm 9.6$
$\text{NO}_3^- - \text{N}$	mg/L	$14.2 \pm 11.8$	$17.6 \pm 11.9$
$\text{PO}_4^{3-}$	mg/L	$26.3 \pm 9.5$	$15.3 \pm 5.5$
$\text{BOD}_5$	mg/L	$328.7 \pm 78.0$	$39 \pm 17.8$
ORP	mV	$79 \pm 85$	$105 \pm 70$

## Hydrothermal liquefaction processes

Hydrothermal liquefaction (HTL) is a promising approach to degrade the wet wastes (such as sludge and microalgae) and recovery energy in the form of biocrude or biochar. In this study, HTL was done for three samples in which two sludge samples (solids content of 17%) were collected from PABR (at ch-1 and ch-2), and the microalgae sample (solids content of 15%) was collected from photobioreactor. Here, the microalgae sample makes a notable comparison with sludge samples in the case of functional group analysis. The experiments were performed in a 304-grade stainless steel batch reactor with a capacity of 25 ml. The reactor was specified as a 25 mL ppl liner that has been used to store the microalgal solution and sludge (Ch-1 and Ch-2), and the reaction occurred inside the liner with high pressure and temperature. The reactor had uniform wall thickness, which allowed the uniform heating of the reactor.

Approximately 15 ml of sample was taken into the reactor in each experimental run under hydrothermal conditions. The reactor was then taken into the muffle furnace and heated at 280 °C temperature for 60 min. After that, the reactor was taken out from the muffle furnace and cooled rapidly to room temperature by circulating water through the reactor before the product collection. Then, the reactor headspace gases were carefully released, and 30 mL of dichloromethane (DCM) was added to collect the liquefaction products. Here, DCM was used for solvent extraction purposes. The DCM not only extracted the organic components from liquid and solid products but also formed a homogeneous mixture with the organic solvents. Then, the mixed sample was collected into four separate centrifuge tubes. Finally, the tubes were centrifuged at 4000 rpm for 10 min in order to separate the phases (He et al. 2018a, b; Xu et al. 2019). After centrifugation, the organic phase dissolved in dichloromethane stays at the bottom, and the aqueous phase stays at the top, and the biochar stays in the middle that separates the organic phase with the aqueous phase. Then, the aqueous phase was carried out of the tube using a pipette. Afterward, the DCM soluble organic phase was taken out through filtering and then moved into a petri dish. Later on, the DCM soluble organic phase was dried at 40 °C for 1 h to evaporate the DCM solvent. Thus, the biocrude would be separated from DCM, and then FTIR analysis was conducted to find out the characteristics. The solids retained on the filter paper which were later dried at 100 °C for 24 h before conducting FTIR analysis (He et al. 2018a, b). This study was focus on the characteristics of the obtained biocrude and biochar, so the gases and aqueous phases were not further characterized.

## FTIR (Fourier transform infrared spectroscopy) analysis

The composition of biocrude and biochar, and the functional group present in biocrude and biochar obtained from microalgae and sludge (Ch-1 and Ch-2) were assessed through FTIR spectroscopy study (Mahapatra and Ramachandra 2013; Prajapati et al. 2013). The FTIR analyses were conducted on biocrude and biochar at room temperature using Shimadzu (IRTracer-100) FTIR spectrophotometer (Ansari et al. 2017b). The extracts from these samples were observed for their functionalities in the spectrogram. The spectra were collected in the mid-IR range from 4000 to 800  $\text{cm}^{-1}$  (at a spectral resolution of 2  $\text{cm}^{-1}$ ), and data were analyzed using Microsoft Excel, irAnalyze-RAMalyze (Lab-Cognition GmbH and Co. KG), and Essential FTIR (Operant LLC).

## Sampling and analysis

In order to investigate the nutrients removal performances in every chamber of the PABR, ammonia-N ( $\text{NH}_3 - \text{N}$ ), nitrate-N ( $\text{NO}_3^- - \text{N}$ ), oxygen redox potential (ORP), orthophosphate ( $\text{PO}_4^{3-}$ ) and chemical oxygen demand (COD) analyses were performed chamber-wise (ch-1–ch-7) according to the standard methods for the Examination of Water and Wastewater (APHA et al. 2005). Also, biochemical oxygen demand (BOD), total nitrogen (TN), pH, electrical conductivity (EC), turbidity were analyzed for raw and effluent samples during the entire experiment.

## Results and discussion

Samples were collected from the sampling port of each reactor chamber and analyzed in the laboratory followed standard methods. In this study, pH, electrical conductivity (EC), turbidity, total nitrogen (TN), biochemical oxygen demand (BOD, 5 days basis) were monitored for raw and effluent samples. The results showed pH  $8.1 \pm 0.2$  and  $8.1 \pm 0.1$ , EC  $2.62 \pm 0.06$  and  $2.53 \pm 0.14$  mS/cm, and turbidity  $414.6 \pm 224.2$  and  $6.74 \pm 4.4$  NTU for raw and effluent samples, respectively.

### Real-time indication of ORP for nutrient removal

Zhao et al. (2016) have been already reported the correlation between the ORP value and nutrient removal performance. When ammonia is oxidized (during nitrification), the reactor will show positive OPR (e.g., mV) reading. On the contrary, negative ORP reading is observed when nitrate is reduced (during denitrification). During the study period, the ORP value was monitored every chamber of PABR (ch-1–ch-7), and the average, maximum, and minimum values are shown in Fig. 3. And the environmental conditions along with the chamber are shown in Table 3. These values indicated that there existed an anoxic/oxic condition in ch-1–ch-3, which is favorable for nitrification and denitrification. ORP value was dropped up to  $-215$  mV in ch-1, indicating anaerobic conditions for  $\text{NO}_3$  depletion and phosphorus released.

**Fig. 3** ORP concentration along with the chamber

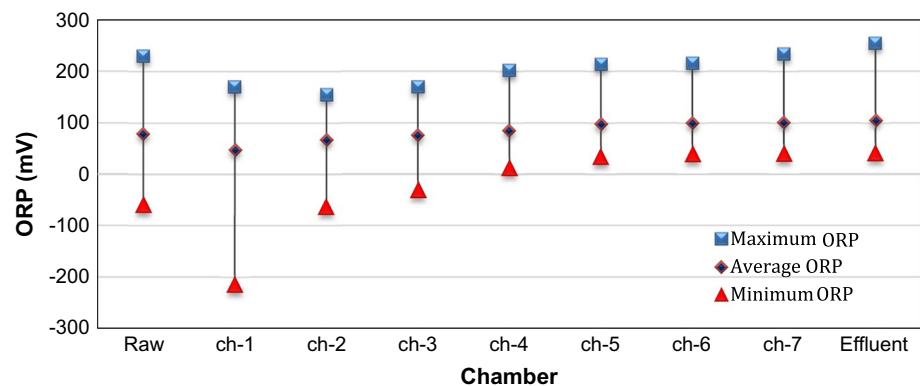


**Table 3** Biological environmental conditions along with the chamber

	Ch-1	Ch-2	Ch-3	Ch-4	Ch-5	Ch-6	Ch-7
ORP range	-215 to +170	-64 to +155	-31 to +170	+12 to +170	+34 to +170	+49 to +170	+50 to +170
Environmental conditions	A/O	A/O	A/O	O	O	O	O
Ammonia-N removal	N/MA	N/MA	N/MA	N/MA	N/MA	N/MA	N/MA
Nitrate-N removal	D/MA	D/MA	D/MA	MA	MA	MA	MA

A anoxic, D denitrification, N nitrification, O oxic, MA microalgal assimilation



Moreover, the ORP values of ch-1–ch-3 clearly indicated that simultaneous nitrification and denitrification (SND) occurred inside these chambers were the main responsible for nitrate–N removal.

On the other hand, the ORP values of ch-4–ch-7 indicated that there existed an oxic environment inside the chambers, which was favorable for nitrification and microalgal assimilation. As ORP value was considered real-time control parameter for SND (Zhao et al. 1999), so it was concluded that ORP value automatically divided the PABR into two unit systems generally consist of an anoxic zone (ch-1–ch-3) and aerobic zone (ch-4–ch-7).

### Organic matter removal

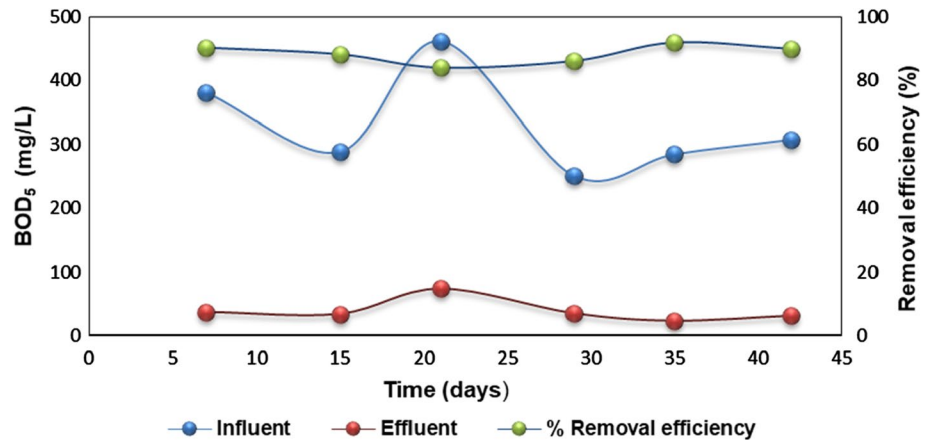
The organic matter present in wastewater is associated with two components, such as dissolved organic matter (soluble BOD) and suspended organic matter (particulate BOD). The part of suspended organic matters (particulate BOD) was settled down at the bottom of the reactor and decomposed by anaerobic microorganisms and converted into carbon dioxide, methane, and other compounds. The non-biodegradable (inert) fractions stayed at the bottom of the reactor. The dissolved organic matters (soluble BOD) did not settle down

and dispersed in the wastewater liquid mass. They were decomposed by facultative microorganisms that have the ability to survive in the present as well as in the absence of dissolved oxygen. In the absence of dissolved oxygen, these facultative bacteria used nitrate as an electron acceptor to degrade the soluble organic matter (anoxic condition).

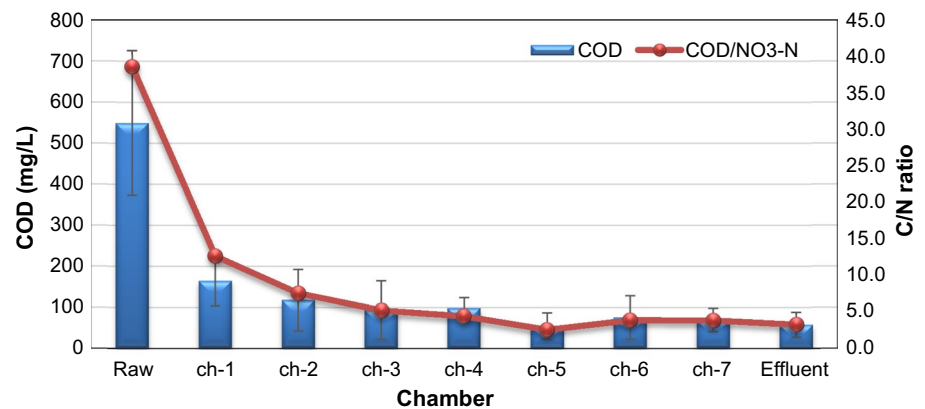
As the actual domestic wastewater was used during the experiments, the influent BOD concentrations were observed to be varying (in Fig. 4). The concentration of influent BOD was varying from 251 to 461 mg/L, and the organic loading rate (OLR) was 0.20–0.37 kg BOD/m<sup>3</sup>/day during the study period of 6 weeks. Figure 4 shows that removal efficiency directly depends on the organic loading rate (OLR). It was noticed that the increase in the organic loading rate (OLR) decreased in removal efficiency (%) (Gopala Krishna et al. 2009).

Figure 5 shows the average COD concentration, and COD/NO<sub>3</sub>-N ratio (C/N ratio) of each chamber as the COD/nitrate ratio significantly affects the biological denitrification process (Chiu and Chung, 2003). It appeared that the COD concentration decreased along with the chambers when the wastewater passed through the ch-1–ch-7. The significant decrease in COD value was observed in the first chamber, as this chamber was

**Fig. 4** Influent and effluent BOD concentration and removal efficiency



**Fig. 5** Chamber-wise variation of COD and C/N ratio



designed as a sedimentation chamber. Most of the organic matter was removed in the first three chambers, and COD removals in the first three chambers were 70, 9, and 4%, in ch-1, ch-2, and ch-3, respectively. The COD concentration of the last four chambers was fluctuated due to biomass washout from these chambers.

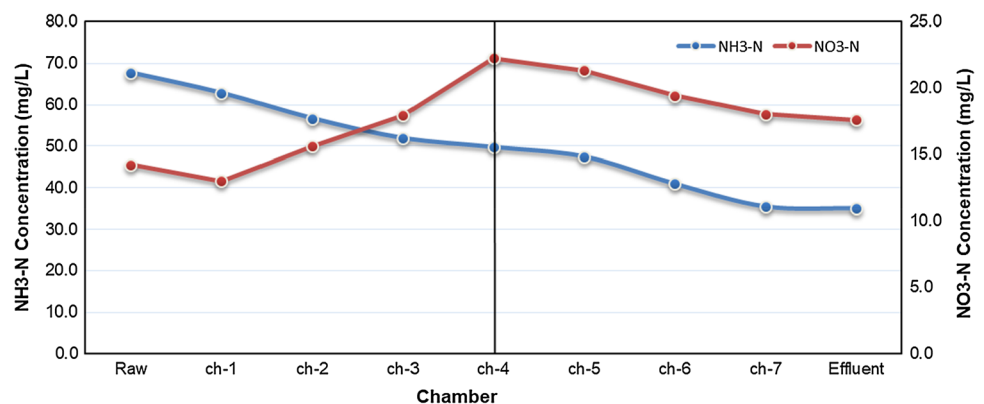
## Nitrogen removal

Nitrification (oxidation of ammonia) and algae assimilation were the main removal mechanism of ammonia-N. Oxygen supplied by microalgal-bacterial consortia was used by nitrifiers during the nitrification process. This is one of the main benefits of using the symbiosis of algae and bacteria in the reactor (Rada-Ariza et al. 2019). The average chamber-wise ammonia-N and nitrate-N concentration is plotted in Fig. 6. It was noticed that the concentration of ammonia-N was reduced down to the chamber of the PABR, but the value significantly fluctuated along with the chamber. The rate of ammonia-N reducing was high in the first three chambers (ch-1–ch-3), then slightly low in the middle chambers (ch-4 and ch-5), and again high in the last two floated media chambers (ch-6 and ch-7). Previously reported by Barber and Stuckey, (2000a) that a linear relationship between ammonia oxidation and mixing rate where ammonia removal improved with increased mixing rate. This indicated that the oxidation of ammonia was increased at a high mixing rate or high turbulence. At the same time, the hydrodynamic behavior of reactor was investigated by Khalekuzzaman et al. (2018a, b) and was reported that the dispersion number (mixing rate) was high in the first three chambers (ch-1–ch-3), then intermediate dispersion number in the middle chambers (ch-4 and ch-5) and no influence of dispersion number was observed in the last two floated filter media chambers (ch-6 and ch-7). As dispersion number was high in the first three chambers (ch-1–ch-3), so high removal of ammonia-N was noticed in the first three chambers rather than middle chambers due to the high oxidation of ammonia-N. On the other hand, the reducing rate of ammonia-N was high in the last two floated

filter media chambers (ch-6 and ch-7) due to the uptake of ammonia-N by algae in the attached growth of algal biofilm inside the floated filter media. And the main ammonia-N removal mechanism in the last chambers was through algae assimilation followed by nitrification, while nitrification was the main ammonia-N removal mechanism in the first three chambers. Moreover, the average effluent ammonia-N was 34.9 mg/L, with the removal efficiency of 48.4%. Also, the ORP value was indicated that every chamber of the reactor was suitable for nitrification and algae assimilation.

On the other hand, nitrate-N was produced in every chamber of the reactor via the nitrification process, where released oxygen during the photosynthesis process was consumed by Nitrosomonas and Nitrobacter bacteria. The concentration of nitrate-N was firstly increased up to ch-4; after that, the concentration was decreased along with the chamber. Raw wastewater was stored in a feeding tank, so during this time, nitrification took place inside the feeding tank. That's why a small quantity of nitrate-N was presented in the raw wastewater. The amount of nitrate-N presence in the chamber depends on the balance of the simultaneous nitrification and denitrification process (Zhang et al. 2007). And the concentration of nitrate-N was high in ch-4, up to 22.3 mg/L. It indicated that the amount of COD required as carbon sources were not enough for denitrification. Chiu and Chung (2003) also pointed out that sufficient COD/NO<sub>3</sub>-N was required to provide enough degradable carbon sources as an electron donor for denitrification. It was noticed in Fig. 5 that the COD/NO<sub>3</sub>-N ratio was very low in the middle two chambers (ch-4 and ch-5), as a result no denitrification occurred in those chambers. As a result, the concentration of nitrate-N was comparatively high in the middle two chambers (ch-4 and ch-5). At the same time, simultaneous nitrification and denitrification (SND) occurred in the first three chambers (ch-1–ch-3) due to the high COD/NO<sub>3</sub>-N ratio; as a result, the concentration of nitrate-N was comparatively lower than other chambers. The efficiency of the SND process in the first three chambers was 125, 58, and 51%, respectively. Although there existed a very low COD/

**Fig. 6** Ammonia-N and nitrate-N concentration along with the chamber



$\text{NO}_3\text{-N}$  ratio in the last two floated filter media chambers, the nitrate–N concentration was reducing due to microbial assimilation of nitrate–N.

However, it was also observed that a very low value of ORP has prevailed only in the first three chambers of the PABR, indicating a suitable environment for denitrification. The rest chambers of the reactor were less effective for denitrification because of the low COD/ $\text{NO}_3\text{-N}$  ratio (Qingjuan et al. 2008). As a result, the concentration of nitrate–N was quite high in the middle chambers. But the concentration of nitrate–N was reduced last two chambers due to microbial assimilation of nitrate–N in the attached growth of algal biofilm inside the floated filter media. In addition, the ORP value of the last four chambers indicated that the chambers of the reactor were suitable for microbial assimilation.

The  $\text{NO}_x\text{-N}$  was produced in every chamber of the PABR via nitrification process, where it was to convert into nitrogen gas or microbial assimilation leading to the TN removal process. Figure 7 shows the TN concentration in both influent and effluent as well as removal efficiencies of the PABR during the study period. The results showed that the total nitrogen removal was not high, either ammonia–N or nitrate–N present in the effluent. As using domestic wastewater, the concentration of total

nitrogen (TN) of the influent significantly fluctuated, and that would affect the TN removal efficiency. The average effluent TN concentration was 50.2 mg/L, with a removal efficiency of 36.8%.

### Phosphate removal

Phosphate (Orthophosphate,  $\text{PO}_4^{3-}$ ) was firstly released in the anoxic zone by the phosphate accumulating organisms (PAOs) and then decreased in the oxic zone due to phosphate uptake by the denitrifying phosphate accumulating organisms (DPAOs) (Wu et al. 2016). The average influent and effluent, as well as the chamber-wise concentration of phosphate, are shown in Fig. 8. The results showed that the concentration of phosphate was decreasing along to the chamber. The average effluent concentration of phosphate was 15.3 mg/L, with a removal efficiency of 42%. However, the pH levels were  $8.0 \pm 0.2$ ,  $8.0 \pm 0.1$ ,  $8.0 \pm 0.1$ ,  $8.0 \pm 0.1$ ,  $8.0 \pm 0.1$ ,  $7.9 \pm 0.2$ , and  $8.0 \pm 0.2$  at ch-1–ch-7, respectively. When the pH value was increased up to 9, the phosphate gets precipitated due to increased pH (Su et al. 2012). Still, this effect is not significant in the present study since the pH level was below 9 during the treatment process.

**Fig. 7** Influent and effluent TN concentration and removal efficiency

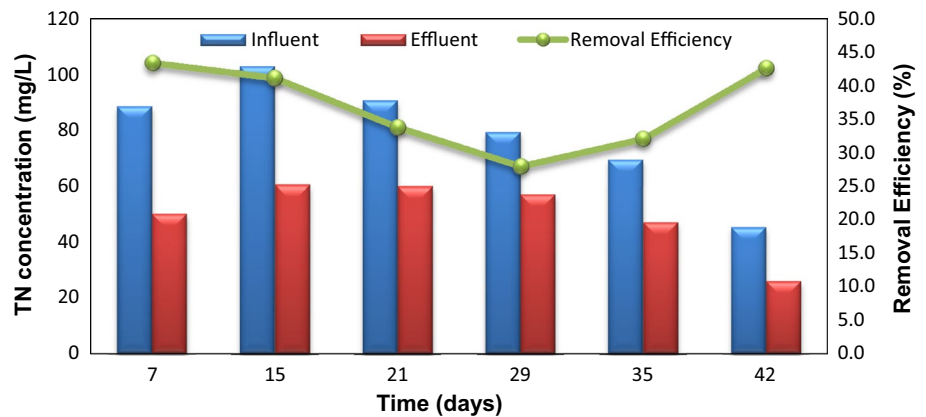
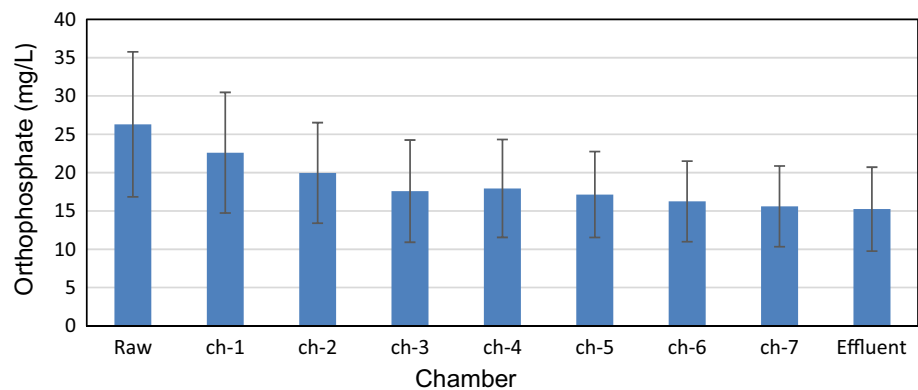


**Fig. 8** Phosphate concentration along with the chamber





## Fourier transform infrared spectroscopy (FTIR) analysis

The FTIR spectroscopic analyses were conducted to observe the distribution of functional groups present in HTL products (biocrude and biochar) (Ansari et al. 2017a). The peaks found in different wavenumbers indicated active functional groups (including  $(\text{CH}_2)_4\text{-C}$ , C–H Stretch,  $-\text{CH}_2/-\text{CH}_3$  Stretch, COO (Esters), C–O–C, C=O, C=C, C–S, N=O) in the biochar and biocrude samples. It was also noticed that all the samples were contaminated with dissolved  $\text{CO}_2$  (at  $2250\text{ cm}^{-1}$ – $2450\text{ cm}^{-1}$ ). After eliminating the dissolved  $\text{CO}_2$  contamination and manual baseline correction, the peaks were analyzed for active functional groups.

### Characterization of biochar

The biochar from HTL of microalgae and sludge samples (Ch-1 and Ch-2) was characterized by FTIR and is presented

**Table 4** FTIR band assignments for biochar of microalgae and sludge samples

Functional groups	Spectra range ( $\text{cm}^{-1}$ )	Strength of spectra ranges		
		Microalgae	Ch-1	Ch-2
C–H Stretch	2900–2975	Variable	Variable	Variable
C–O	1070–1100	Strong	Strong	Strong
N=O	1500–1580	Strong	Strong	Strong
N–H Deformation	800–870	Variable	Variable	Variable
C=C, trans	1640–1690	Medium	Medium	Medium
N–H	1560–1640	Strong	Strong	Strong
Si–O Stretch	1000–1100	Strong	Strong	Strong
C–N Stretch	1035–1070	Variable	Variable	Variable
C=O	1700–1755	Variable	Variable	Variable

in Fig. 9 and Table 4. The sludge samples showed almost similar peaks, but the difference was found when compared to the microalgal biochar sample. Again, the peak intensity

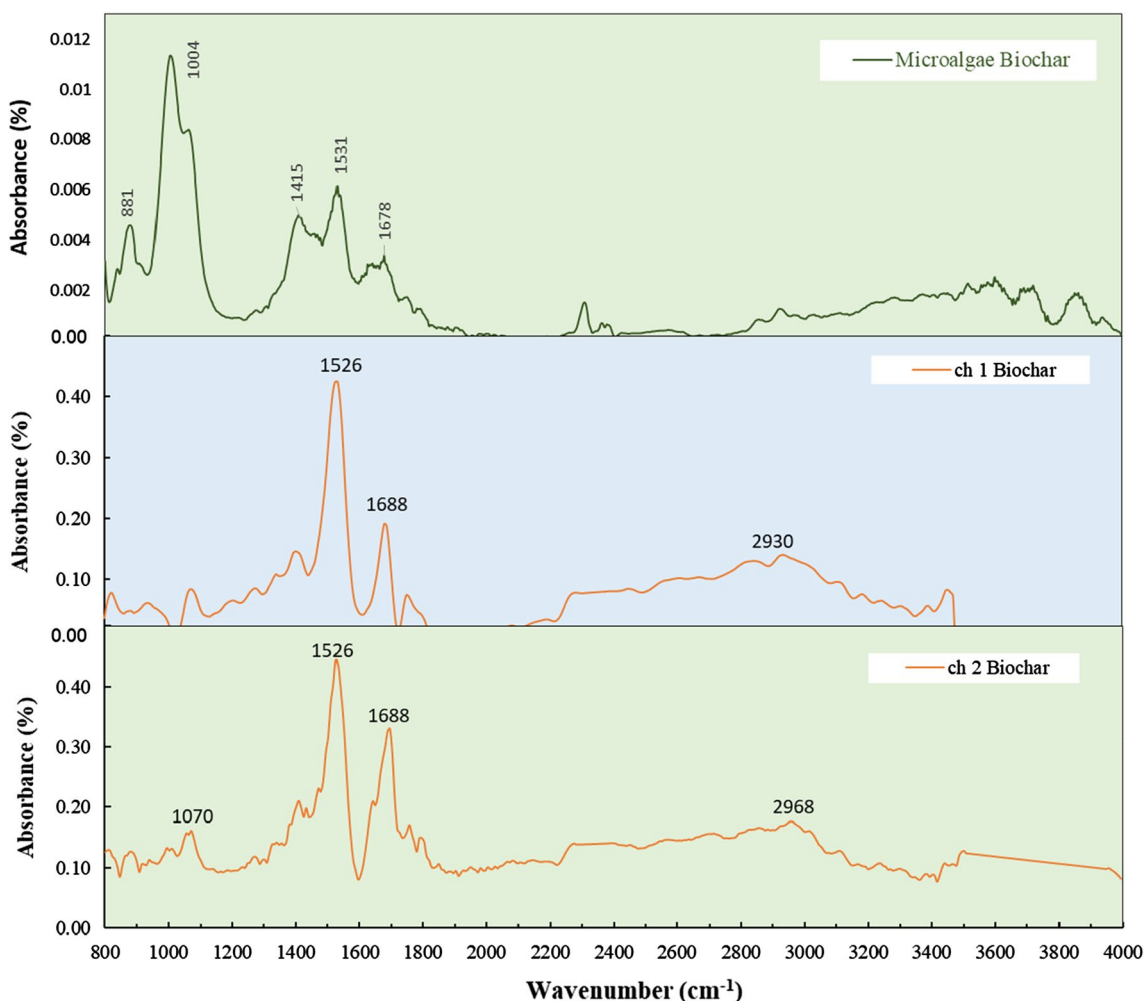


**Fig. 9** FTIR absorbance spectroscopy on biochar samples of microalgae and sludge after hydrothermal liquefaction



for sludge biochar was very stronger than microalgal biochar. The peak occurring at  $2860\text{--}2970\text{ cm}^{-1}$ , which indicates the C–H alkyl functional groups, was almost absent in the biochar samples. Both microalgae and sludge biochar samples showed peaks at the range  $1640\text{--}1690\text{ cm}^{-1}$  and  $1500\text{--}1580\text{ cm}^{-1}$ , which denoted the C=C and N=O stretching of p-nitrophenol compound (Mahapatra and Ramachandra 2013). Both the microalgae biochar and sludge biochar samples showed peaks for Si–O/C–O (at  $1000\text{--}1100\text{ cm}^{-1}$ ), which is presented in the microalgae outer cell membrane (Si–O–C) (Annenkov et al. 2015). So, the sludge might contain microalgae cells in them. The sludge samples also showed peaks for the C–C ring (at  $1475\text{--}1505\text{ cm}^{-1}$ ), C–N stretching (at  $1035\text{--}1070\text{ cm}^{-1}$ ), and N–H stretching (at  $1560\text{--}1640\text{ cm}^{-1}$ ) which proved the presence of aromatic nitrile, aliphatic amine salt, and N-methyl amino compound. The researchers also found the same functional groups for FTIR of biochar (Lu et al. 2018; Jena et al. 2012; Vardon et al. 2011). The presence of nitrogen compounds in the sludge biochar samples suggested that it could be utilized to make fertilizers.

### Characterization of biocrude

The FTIR analysis and the spectroscopy of biocrude oil from sludge (Ch-1 and Ch-2) and microalgae are illustrated in Fig. 10 and Table 5. Similar peaks were observed in both biocrude samples with long-chain alkyl hydrocarbons ( $2916\text{--}2936\text{ cm}^{-1}$ ,  $2845\text{--}2975\text{ cm}^{-1}$ ,  $1360\text{--}1390\text{ cm}^{-1}$ ,  $1415\text{--}1475\text{ cm}^{-1}$ ). Moreover, when comparing with microalgal biocrude, the peaks for sludge biocrude were 32 times more intense. The peaks at  $1080\text{--}1135\text{ cm}^{-1}$ ,  $1640\text{--}1800\text{ cm}^{-1}$ , and  $1470\text{--}1590\text{ cm}^{-1}$  represented the C–O, C=O, and C=C ring stretching of aromatic carboxylic acid. The  $1050\text{ cm}^{-1}$  and  $1557\text{ cm}^{-1}$  peaks denoted the C–N and N–H stretching of the amino group. The carbonyl compound was observed at peaks for the wavelength of  $1720\text{--}1770\text{ cm}^{-1}$ . These chemical compounds presented in biocrude were observed by many researchers (Guo et al. 2015; Lu et al. 2018; Vardon et al. 2011).

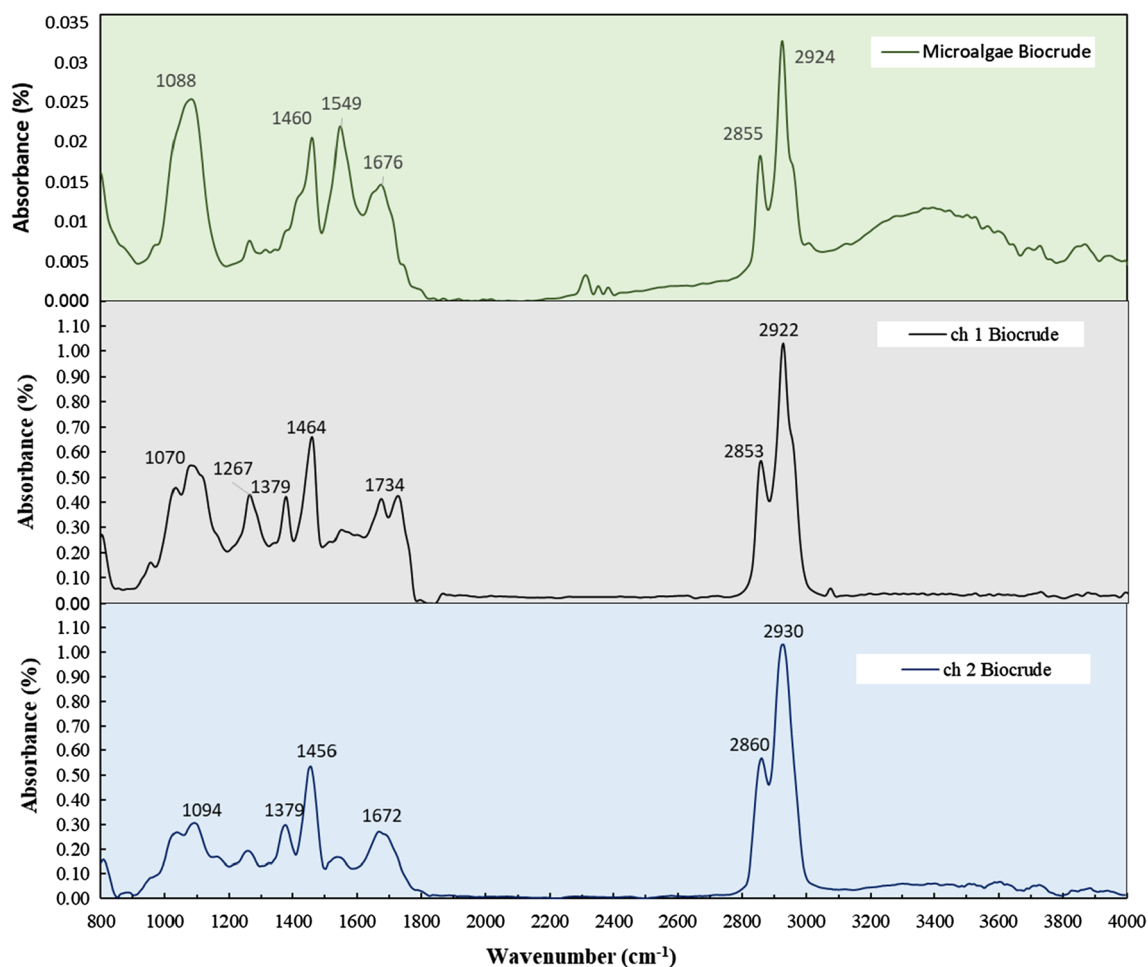


**Fig. 10** FTIR absorbance spectroscopy on biocrude samples of microalgae and sludge after hydrothermal liquefaction



**Table 5** FTIR band assignments for biocrude of microalgae and sludge samples

Functional groups	Spectra range (cm <sup>-1</sup> )	Strength of spectra ranges		
		Microalgae	Ch-1	Ch-2
(CH <sub>2</sub> ) <sub>4</sub> -C	2916–2936	Medium	Strong	Strong
C–H Stretch, Alkyl	2845–2975	Variable	Strong	Strong
CH <sub>2</sub> /CH <sub>3</sub> Stretch	1415–1475	Variable	Variable	Variable
	1360–1390	Variable	Variable	Variable
C=O	1640–1800	Variable	Variable	Variable
COO(Esters)	1720–1770	–	Variable	Variable
C–O–C	1100–1300	Medium	Strong	Strong
C–O	1070–1135	Strong	Strong	Strong
N=O	1500–1580	Variable	–	–
C–N Stretch	1060–1080	Variable	Variable	Variable
C=C ring stretch	1470–1590	Variable	Variable	Variable
C–S=O	1020–1060	Strong	Strong	Strong
Si–O Stretch	1000–1100	Very strong	Very strong	Very strong

## Conclusion

This study investigated the combined effect of microalgae–bacteria consortium in removing nutrient and organic matter from domestic wastewater. An average BOD, NH<sub>3</sub>-N, TN, and phosphate removal efficiencies were more than 88, 48, 36, and 42%, respectively. The ORP values indicated that the reactor was automatically divided into two unit systems that generally consist of an anoxic zone (ch-1–ch-3) and aerobic zone (ch-4–ch-7) due to the unique compartmentalized structure of the PABR. Simultaneous nitrification/denitrification (SND) and microbial assimilation were the main nutrients removal mechanism in the PABR where nutrients removed by SND occurred in the first three chambers, and microbial assimilation was governed in the last four chambers. The experimental results of the PABR show that the algal–bacterial symbiosis system was more effective for organic waste removal and partially effective for nutrients removal. But this problem can be resolved by increasing the light intensity and hydraulic retention time (HRT). Moreover, the sludge accumulated from PABR was converted into biocrude and biochar by HTL process. The FTIR analysis suggests that the biocrude and biochar derived from sludge are better than that of microalgae.

## Compliance with ethical standards

**Conflict of interest** The authors declared that there are no conflicts of interest.

**Open Access** This article is licensed under a Creative Commons Attribution 4.0 International License, which permits use, sharing, adaptation, distribution and reproduction in any medium or format, as long as you give appropriate credit to the original author(s) and the source, provide a link to the Creative Commons licence, and indicate if changes were made. The images or other third party material in this article are included in the article's Creative Commons licence, unless indicated otherwise in a credit line to the material. If material is not included in the article's Creative Commons licence and your intended use is not permitted by statutory regulation or exceeds the permitted use, you will need to obtain permission directly from the copyright holder. To view a copy of this licence, visit <http://creativecommons.org/licenses/by/4.0/>.

## References

- Alcántara C, Domínguez JM, García D, Blanco S, Pérez R, García-Encina PA, Muñoz R (2015) Evaluation of wastewater treatment in a novel anoxic–aerobic algal–bacterial photobioreactor with biomass recycling through carbon and nitrogen mass balances. *Biores Technol* 191:173–186. <https://doi.org/10.1016/j.biortech.2015.04.125>
- Annenkov VV, Pal'shin VA, Verkhovzina ON, Larina LI, Danilovtseva EN (2015) Composite nanoparticles: a new way to siliceous materials and a model of biosilica synthesis. *Mater Chem Phys* 165:227–234. <https://doi.org/10.1016/j.matchemphys.2015.09.022>
- Ansari AA, Khoja AH, Nawar A, Qayyum M, Ali E (2017) Wastewater treatment by local microalgae strains for CO<sub>2</sub> sequestration and biofuel production. *Appl Water Sci* 7(7):4151–4158. <https://doi.org/10.1007/s13201-017-0574-9>
- APHA, Awwa, AEF (2005) Standard methods for the examination of water and wastewater. American Public Health Association, USA
- Barber WP, Stuckey DC (2000a) Nitrogen removal in a modified anaerobic baffled reactor (ABR): 1, denitrification. *Water Res* 34(9):2413–2422
- Barber WP, Stuckey DC (2000b) Nitrogen removal in a modified anaerobic baffled reactor (ABR): 2, nitrification. *Water Res* 34(9):2423–2432. [https://doi.org/10.1016/S0043-1354\(99\)00426-1](https://doi.org/10.1016/S0043-1354(99)00426-1)
- Boelee NC, Temmink H, Janssen M, Buisman CJN, Wijffels RH (2012) Scenario analysis of nutrient removal from municipal wastewater by microalgal biofilms. *Water* 4(2):460–473. <https://doi.org/10.3390/w4020460>
- Chen Z, Wen Q, Guan H, Bakke R, Ren N (2014) Anaerobic treatment of domestic sewage in modified septic tanks at low temperature. *Environ Technol* 35(17):2123–2131. <https://doi.org/10.1080/09593330.2014.894580>
- Chiu YC, Chung MS (2003) Determination of optimal COD=nitrate ratio for biological denitrification. *Int Biodeterior*. [https://doi.org/10.1016/S0964-8305\(02\)00074-4](https://doi.org/10.1016/S0964-8305(02)00074-4)
- Delgadillo-Mirquez L, Lopes F, Taïdi B, Pareau D (2016) Nitrogen and phosphate removal from wastewater with a mixed microalgae and bacteria culture. *Biotechnol Rep* 11:18–26. <https://doi.org/10.1016/j.btre.2016.04.003>
- Feng H, Hu L, Mahmood Q, Fang C, Qiu C, Shen D (2009) Effects of temperature and feed strength on a carrier anaerobic baffled reactor treating dilute wastewater. *Desalination* 239(1–3):111–121. <https://doi.org/10.1016/j.desal.2008.03.011>
- Gopala Krishna GVT, Kumar P, Kumar P (2009) Treatment of low-strength soluble wastewater using an anaerobic baffled reactor (ABR). *J Environ Manage* 90(1):166–176. <https://doi.org/10.1016/j.jenvman.2007.08.017>
- Guo Y, Song W, Lu J, Ma Q, Xu D, Wang S (2015) Hydrothermal liquefaction of cyanophyta: evaluation of potential bio-crude oil production and component analysis. *Algal Res* 11:242–247



- He Q, Chen L, Zhang S, Chen R, Wang H, Zhang W, Song J (2018a) Natural sunlight induced rapid formation of water-born algal-bacterial granules in an aerobic bacterial granular photo-sequencing batch reactor. *J Hazard Mater* 359:222–230. <https://doi.org/10.1016/j.jhazmat.2018.07.051>
- He Z, Xu D, Liu L, Wang Y, Wang S, Guo Y, Jing Z (2018b) Product characterization of multi-temperature steps of hydrothermal liquefaction of *Chlorella* microalgae. *Algal Res* 33:8–15
- Jena J, Nayak M, Panda HS, Pradhan N, Sarika C, Panda PK, Rao B, Prasad RB, Sukla LB (2012) Microalgae of Odisha coast as a potential source for biodiesel production. *World Environ* 2(1):11–16
- Kassab G, Halalshah M, Klapwijk A, Fayyad M, van Lier JB (2010) Sequential anaerobic–aerobic treatment for domestic wastewater—a review. *Biores Technol* 101(10):3299–3310. <https://doi.org/10.1016/j.biortech.2009.12.039>
- Khalekuzzaman M, Alamgir M, Hasan M, Hasan MN (2018a) Performance comparison of uninsulated and insulated hybrid anaerobic baffled reactor (HABR) operating at warm temperature. *Water Sci Technol*. <https://doi.org/10.2166/wst.2018.401>
- Khalekuzzaman M, Hasan M, Haque R, Alamgir M (2018b) Hydrodynamic performance of a hybrid anaerobic baffled reactor (HABR): effects of number of chambers, hydraulic retention time, and influent temperature. *Water Sci Technol* 78(4):968–981. <https://doi.org/10.2166/wst.2018.379>
- Khalekuzzaman Md, Alamgir M, Islam MdB, Hasan M (2019) A simplistic approach of algal biofuels production from wastewater using a Hybrid Anaerobic Baffled Reactor and Photobioreactor (HABR-PBR) system. *PLoS ONE* 14(12):e0225458. <https://doi.org/10.1371/journal.pone.0225458>
- Lee Y-J, Lei Z (2019) Microalgal-bacterial aggregates for wastewater treatment: a mini-review. *Bioresour Technol Rep*. <https://doi.org/10.1016/j.biteb.2019.100199>
- Lu J, Watson J, Zeng J, Li H, Zhu Z, Wang M, Zhang Y, Liu Z (2018) Biocrude production and heavy metal migration during hydrothermal liquefaction of swine manure. *Process Saf Environ Prot* 115:108–115
- Mahapatra DM, Ramachandra TV (2013) Algal biofuel: bountiful lipid from *Chlorococcum* sp. proliferating in municipal wastewater. *Current Sci* 105(1):47–55
- Medina M, Neis U (2007) Symbiotic algal bacterial wastewater treatment: effect of food to microorganism ratio and hydraulic retention time on the process performance. *Water Sci Technol* 55(11):165–171. <https://doi.org/10.2166/wst.2007.351>
- Meng Q, Yang F, Liu L, Meng F (2008) Effects of COD/N ratio and DO concentration on simultaneous nitrification and denitrification in an airlift internal circulation membrane bioreactor. *J Environ Sci* 20(8):933–939
- Mohd Aris MA, Chelliapan S, Md Din MF, Nor Anwar A, Shahperi R, Bannir Selvam S (2016) Effect of effluent circulation and hydraulic retention time (HRT) on the performance of a modified anaerobic baffled reactor (MABR) during start-up period. *Desalin Water Treat* 57(40):18597–18605. <https://doi.org/10.1080/19443994.2015.1094676>
- Nguyen TDP, Le TVA, Show PL, Nguyen TT, Tran MH, Tran TNT, Lee SY (2019) Bioflocculation formation of microalgae-bacteria in enhancing microalgae harvesting and nutrient removal from wastewater effluent. *Biores Technol* 272:34–39. <https://doi.org/10.1016/j.biortech.2018.09.146>
- Ponnuswamy I, Madhavan S, Shabudeen S (2013) Isolation and characterization of green microalgae for carbon sequestration, waste water treatment and bio-fuel production. *Int J Bio-Sci Bio-Technol* 5(2):17–26
- Prajapati SK, Kaushik P, Malik A, Vijay VK (2013) Phycoremediation and biogas potential of native algal isolates from soil and wastewater. *Biores Technol* 135:232–238. <https://doi.org/10.1016/j.biortech.2012.08.069>
- Quijano G, Arcila JS, Buitrón G (2017) Microalgal-bacterial aggregates: applications and perspectives for wastewater treatment. *Biotechnol Adv* 35(6):772–781. <https://doi.org/10.1016/j.biotechadv.2017.07.003>
- Rada-Ariza AM, Lopez-Vazquez CM, van der Steen NP, Lens PNL (2017) Nitrification by microalgal-bacterial consortia for ammonium removal in flat panel sequencing batch photo-bioreactors. *Biores Technol* 245:81–89. <https://doi.org/10.1016/j.biortech.2017.08.019>
- Rada-Ariza AM, Fredy D, Lopez-Vazquez CM, Van der Steen NP, Lens PNL (2019) Ammonium removal mechanisms in a microalgal-bacterial sequencing-batch photobioreactor at different solids retention times. *Algal Res* 39:101468. <https://doi.org/10.1016/j.algal.2019.101468>
- Rongrong L, Qing T, Jihua C (2010) The developments of anaerobic baffled reactor for wastewater treatment: A review. *Afr J Biotech* 9(11):1535–1542. <https://doi.org/10.5897/AJB10.036>
- Sabumon PC (2008) Development of a novel process for anoxic ammonia removal with sulphidogenesis. *Process Biochem* 43(9):984–991. <https://doi.org/10.1016/j.procbio.2008.05.004>
- Saby S, Djafer M, Chen G-H (2003) Effect of low ORP in anoxic sludge zone on excess sludge production in oxic-settling-anoxic activated sludge process. *Water Res* 37(1):11–20. [https://doi.org/10.1016/S0043-1354\(02\)00253-1](https://doi.org/10.1016/S0043-1354(02)00253-1)
- Su Y, Mennerich A, Urban B (2012) Synergistic cooperation between wastewater-born algae and activated sludge for wastewater treatment: Influence of algae and sludge inoculation ratios. *Biores Technol* 105:67–73. <https://doi.org/10.1016/j.biortech.2011.11.113>
- Tiron O, Bumbac C, Manea E, Stefanescu M, Nita Lazar M (2017) Overcoming microalgae harvesting barrier by activated algae granules. *Scientific Reports*. <https://doi.org/10.1038/s41598-017-05027-3>
- Vardon DR, Sharma BK, Scott J, Yu G, Wang Z, Schideman L, Zhang Y, Strathmann TJ (2011) Chemical properties of biocrude oil from the hydrothermal liquefaction of *Spirulina* algae, swine manure, and digested anaerobic sludge. *Biores Technol* 102(17):8295–8303
- Wu P, Peng Q, Xu L, Wang J, Huang Z, Zhang J, Shen Y (2016) Effects of temperature on nutrient removal performance of a pilot-scale ABR/MBR combined process for raw wastewater treatment. *Desalin Water Treat* 57(26):12074–12081. <https://doi.org/10.1080/19443994.2015.1048741>
- Xu D, Wang Y, Lin G, Guo S, Wang S, Wu Z (2019) Co-hydrothermal liquefaction of microalgae and sewage sludge in subcritical water: Ash effects on bio-oil production. *Renew Energy* 138:1143–1151. <https://doi.org/10.1016/j.renene.2019.02.020>
- Zhang X, Zhou J, Guo H, Qu Y, Liu G, Zhao L (2007) Nitrogen removal performance in a novel combined biofilm reactor. *Process Biochem* 42(4):620–626. <https://doi.org/10.1016/j.procbio.2006.11.012>
- Zhao HW, Mavrinic DS, Oldham WK, Koch FA (1999) Controlling factors for simultaneous nitrification and denitrification in a two-stage intermittent aeration process treating domestic sewage. *Water Res* 33(4):961–970. [https://doi.org/10.1016/S0043-1354\(98\)00292-9](https://doi.org/10.1016/S0043-1354(98)00292-9)
- Zhao W, Zhang Y, Lv D, Wang M, Peng Y, Li B (2016) Advanced nitrogen and phosphorus removal in the pre-denitrification anaerobic/anoxic/aerobic nitrification sequence batch reactor (pre-A 2 NSBR) treating low carbon/nitrogen (C/N) wastewater. *Chem Eng J* 302:296–304. <https://doi.org/10.1016/j.cej.2016.05.012>
- Zhu G, Zou R, Jha AK, Huang X, Liu L, Liu C (2015) Recent developments and future perspectives of anaerobic baffled bioreactor for wastewater treatment and energy recovery. *Crit Rev Environ Sci Technol* 45(12):1243–1276. <https://doi.org/10.1080/10643389.2014.924182>